Scientia Iranica D (2012) 19 (6), 1802–1809

SCIENTIA IRANICA

Sharif University of Technology

Scientia Iranica

Transactions D: Computer Science & Engineering and Electrical Engineering

www.sciencedirect.com

Thinning of concentric two-ring circular array antenna using fire fly algorithm

B. Basu [a], **G.K. Mahanti** [b,*]

[a] Department of Electronics and Communication Engineering, National Institute of Technology, Yupia, Arunachal Pradesh-791112, India
[b] Department of Electronics and Communication Engineering, National Institute of Technology, Durgapur-713209, India

Received 23 October 2011; revised 3 May 2012; accepted 23 June 2012

KEYWORDS
Uniform Concentric Circular Arrays (UCCA);
Fire Fly Algorithm (FFA);
Particle Swarm Optimization (PSO);
Differential Evolution (DE);
Thinning;
First Null Beam Width (FNBW).

Abstract The paper describes the application of novel meta-heuristics of the fire fly algorithm for reduction of the maximum Side Lobe Level (SLL) with specific First Null Beam Width (FNBW) of thinned two-ring Uniform Concentric Circular Arrays (UCCA) of isotropic elements. The effect of thinning is analyzed in the four subsequent examples using uniform and non-uniform excitations for different FNBW. Optimization is carried out without and with prefixing the value of the percentage of thinning. The UCCA containing 35 and 70 elements in the two successive concentric rings is optimized using FFA. The example using non-uniform excitation is proved more efficient to reduce SLL for same FNBW. Simulation results show the SLL performance improves as we chose the FNBW wider in the designing problem. Fixing the percentage of thinning at a higher value increases the power efficiency of the feeding network with little compromise on the design specifications. The non-uniformly excited thinned concentric array is again optimized using two more state-of-the-art algorithms, namely, Particle Swarm Optimization (PSO) and Differential Evolution (DE) to compare the effectiveness of each algorithm in a statistically meaningful way. Design results using fire fly algorithm shows better performances compared to PSO and DE provided the same number of function evaluation has been considered for all the algorithms.

1. Introduction

Thinning an array means turning off some elements in a uniformly spaced or periodic array to create a desired amplitude density across the aperture. An element connected to the feed network is "on", and an element connected to a matched or dummy load is "off". Thinning an array to produce low side lobes is much simpler than the more general problem of non-uniform spacing of the elements [1,2]. Thinning approaches proposed for linear arrays as reported in the literature [1,2] can be well extended in the study of circular arrays. Circular array has several advantages over linear ones, such as it has all-azimuth scan capability and keeps the beam pattern invariant in every ϕ cuts. The purpose of this paper is to analyze the composite array consists of concentric circular rings with equally spaced elements on each circular array.

There is an abundant open literature describing the performances of Uniform Concentric Circular Arrays (UCCA) [3–6]. Steams et al. [3] approximated the Chebyshev radiation pattern function as a truncated Fourier–Bessel series, from which the current amplitude of each circle is obtained.

Goto and Cheng [4] obtain concentric ring arrays sampling a circular aperture distribution. The technique uses a circular aperture with a Taylor distribution [4].

Dessouky et al. [5] describes the array performance in terms of beam power pattern, side lobe level, and beam width in two cases of central element feeding.

Fallahi and Roshandel [6] present a detail analysis of the improvement of the SIR of CA and CCAA by using circular patch antenna.

The thinned concentric circular arrays with uniform amplitude excitations ensure higher power efficiency and beam-forming networks of reduced complexity. However, the uses of

* Corresponding author. Tel.: +91 9474600384.
E-mail addresses: basu_banani@yahoo.in (B. Basu), gautammahanti@yahoo.com (G.K. Mahanti).
Peer review under responsibility of Sharif University of Technology.

ELSEVIER Production and hosting by Elsevier

1026-3098 © 2012 Sharif University of Technology. Production and hosting by Elsevier B.V. Open access under CC BY-NC-ND license.
doi:10.1016/j.scient.2012.06.030

non-uniform amplitude excitations increase the number of degrees of freedom, and thereby improve the array performances as regards side lobe level.

The design of thinned antenna arrays with large number of radiating elements is a difficult task. It involves solving of complex, non-linear, and non-differentiable functions demanding efficient numerical techniques for their solution. Some of the numerically intensive methods are based on perturbation technique, linear programming, dynamic programming, and the Mini–Max approach [7–11]. In recent years, stochastic techniques, such as Genetic Algorithms [7], Particle swarm Optimization [8,9], Invasive weed optimization [10], and differential evolution [11] have been fairly successful at designing antenna arrays having complex array geometries.

Synthesis of thinned concentric ring array using stochastic algorithms is reported in the article [12,13]. Haupt [12] presents thinned concentric array design using GA where modified PSO is used to optimize literature [13].

In this communication we present the method of optimization of the uniformly spaced concentric circular array using an improved variant of a recently proposed meta-heuristic algorithm called fire fly algorithm [14–16]. Radiation beams are synthesized with minimum relative side lobe level and specific FNBW. Four examples are presented: first one optimizes the position of the turned on elements of the uniformly weighted array and FNBW is kept within 10°. Next designing instance calculates the non-uniform excitations as well as turned on element distributions for same FNBW. The case is again repeated for a wider FNBW limited up to 20° in the third example. The optimally thinned array with tapering amplitude distribution with FNBW not more than 10° and 50% level of thinning is considered in the last instance. The elements of the array are assumed to be isotropic radiators and excitation current phases are all constant.

The paper uses two more evolutionary optimization techniques like PSO and DE algorithms to accommodate one of the four antenna designing instances. Simulation results obtained in each case using all the three algorithms are compared in a statistically significant way.

2. Uniform concentric circular arrays

Figure 1 represents a two-ring uniform concentric circular array with N_m equally spaced isotropic elements along the circle of radius r_m ($m = 1, 2$). The inter element spacing d_m in each ring is half of the signal wavelength to be operated by the array. The radius and angular position of each element in the array is $r_m = N_m\lambda/4\pi$ and $\phi_{mn} = 2n\pi/N_m$, respectively.

The radiation pattern in the plane of the array is given by [17]:

$$E(\theta,\phi) = \sum_{m=1}^{2}\sum_{n=1}^{N_m} I_{mn} e^{jkr_m[\sin\theta\cos(\phi-\phi_{mn}) - \sin\theta_0\cos(\phi_0-\phi_{mn})]}. \tag{1}$$

I_{mn} = Excitation of nth element in the mth ring.

θ = is the elevation angle measured between the positive z-axis and the point of the far field. ϕ is the azimuth angle between the positive x-axis and the projection of the far-field point in the x–y plane as shown in Figure 1.

θ_0, ϕ_0 = direction at which main beam achieves its maximum. For all the designing problems we consider $\theta_0 = 0°$ and $\phi_0 = 0°$.

k = wave number $= 2\pi/\lambda$.

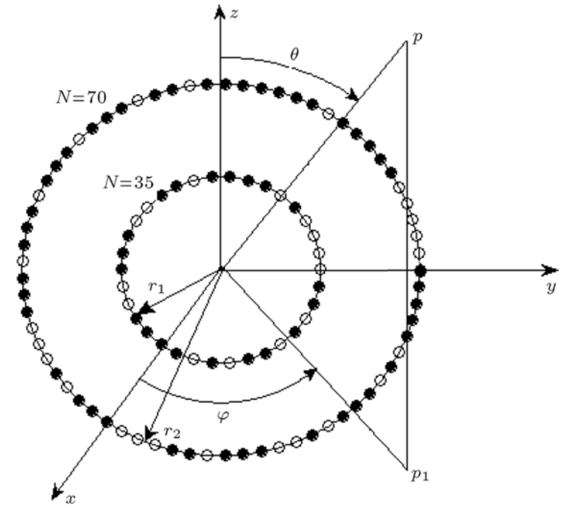

Figure 1: Thinned two-ring array of isotropic elements in *XY* plane.

Normalized power pattern in dB can be expressed as follows:

$$P(\theta,\phi) = 10\log_{10}\left[\frac{|E(\theta,\phi)|}{|E(\theta,\phi)|_{\max}}\right]^2 = 20\log_{10}\left[\frac{|E(\theta,\phi)|}{|E(\theta,\phi)|_{\max}}\right]. \tag{2}$$

Optimization task in the four antenna designing problems is modeled as a minimax problem: minimization of maximum SLL subjected to numerous designing restrictions. First problem uses uniform excitation where rests are non-uniformly excited. First three design instances consider different values of FNBW as optimization constraint. However, last problem is synthesized for a fixed level of thinning percentage and FNBW. Fitness functions are formulated to meet the corresponding designing goals as follows. We consider our design at $\phi = 0$ plane.

$$\text{Fit 1} = \begin{cases} \max(\text{SLL}) & \text{if } \text{FNBW}_o < \text{FNBW}_d \\ 10^2 & \text{otherwise} \end{cases} \tag{3}$$

$$\text{Fit 3} = \begin{cases} \max(\text{SLL}) + (\text{Th}_o - \text{Th}_d)^2 & \text{if } \text{FNBW}_o < \text{FNBW}_d \\ 10^2 & \text{otherwise.} \end{cases} \tag{4}$$

FNBW_o and FNBW_d are the obtained and desired values of the first null beam width. Th_o and Th_d are the obtained and desired values of percentage of thinning.

3. Overview of fire fly algorithm

Xin-She Yang developed the Fire Fly Algorithm (FFA) [15] for solving continuous constrained optimization problems. The algorithm is inspired by the flashing behavior of the fireflies and based on the assumption that the solution of the optimization problem can be perceived as a firefly which glows proportionally to its quality in the considered problem setting [14–16]. Consequently less bright fly being attracted by the brighter one moves toward it and thus it keeps changing its position to explore the entire search space.

Proposed algorithm may be summarized as follows.

(a) *Initialize swarm*: A finite number of fireflies are initialized randomly in the d dimensional search space. These initial solutions are further improved through an iterative process which stops when the best solution has been found, or the maximum number of iterations n has been reached.

FFA uses N d dimensional parameter vectors as population for each generation. The initial population x_i $(i = 1, 2, \ldots, N)$ is initialized randomly within the search space so that $l_b \leq x_i \leq u_b$ where $S = [l_b, u_b]$, i.e. search space is bounded with the specific maxima and minima l_b and u_b, respectively.

(b) *Calculation of light intensity*: The meta-heuristic relies on the initial set of fireflies that communicate with each other by emitting flashing light. Fireflies are characterized by their attractiveness and the light intensity emitted by itself. Light intensity, I_i, of any vector is proportional to the inverse of the fitness value associated with each solution.

$$I_i = 1/f(x_i). \tag{5}$$

(c) *Calculation of attractiveness*: Attractiveness can be adjusted by modifying two parameters: its maximum value β_0 and an absorption coefficient γ.

In general $\beta_0 \in [0, 1]$. We consider two limiting values of β_0 : $\beta_0 = 0$ indicates non-cooperative distributed random search and $\beta_0 = 1$ signifies cooperative local search where brightest firefly determines the positions of the other fireflies in its own neighborhood [15]. It is desirable to chose the maximum attractiveness value $\beta_0 = 1$.

On the other hand, the value of γ determines the variation of attractiveness as a function of distances between the communicated fireflies. $\gamma = 0$ corresponds to no variation or constant attractiveness and conversely $\gamma = 1$ results in an attractiveness close to zero which again is equivalent to the complete random search. We prefer to keep the value of $\gamma \in [0, 1]$.

Attractiveness of any population x_i is determined using the monotonically decreasing function described by:

$$\beta = (\beta_0 - \beta_{\min})e^{-\gamma r_j^2}. \tag{6}$$

r_j is the distances between ith and an arbitrarily chosen jth parameter vector where $j \in \{1, 2, \ldots, N\}$ and $j \neq i$.

(d) *Generation of new swarm*: New solution is generated by the attractiveness of the swarm member with higher intensity.

For each ith solution if there exist any x_j such that $I_j > I_i$ where $j \in \{1, 2, \ldots, N\}$ and $j \neq i$, ith solution changes its position according to:

$$x_i = x_i + \beta(x_j - x_i) + u_i. \tag{7}$$

β controls the amplification of the differential variation $(x_i - x_j)$. u_i is the randomly chosen step size added to increase the diversity of the perturbed solution.

If no brighter solution is found, then only this randomized step is used to generate new solution

$$x_i(t+1) = x_i(t) + u_i. \tag{8}$$

Finally we define the random step size u_i for each search space dimension, k.

$$u_{ik} = \begin{cases} \alpha \text{ rand } 1(1,d)(b_k - x_{i,k}) \\ \quad \text{if } \operatorname{sgn}(\text{rand } 2 - 0.5) < 0 \\ -\alpha \text{ rand } 1(1,d)(x_{i,k} - a_k) \\ \quad \text{if } \operatorname{sgn}(\text{rand } 2 - 0.5) \geq 0 \end{cases} \tag{9}$$

$[a_k, b_k] \in S\ \forall k = 1, 2, \ldots, n$. Random step size u_i has a lower and upper bound and depends on the algorithm parameter α. The absolute value of the range of the dynamic search space adds an envelope to u_i. Here rand $1(1, d)$ is a 1-by-d vector with uniformly distributed random number between 0 and 1 and rand 2 is a uniformly distributed random number between 0 and 1.

In standard fire fly algorithm the value of the control parameter α is chosen as a real constant and $\alpha \in (0, 1)$. In this article, we adapt the value of α associated with each population. The key sense of this adaptation is that if α is higher, larger the value of u_i will be selected to explore larger search volume. However, as the algorithm approaches to its optima with iterations the value of α decreases to give smaller value of u_i so that it may undergo a fine search within the smaller neighborhood. Thus a balance is maintained between exploration and exploitation to prevent premature convergence. Eq. (10) presents the updating strategy of α at iteration k.

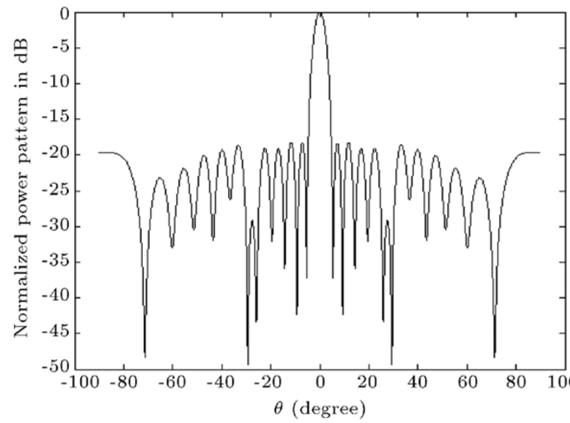

Figure 2: Normalized power pattern of the thinned two-ring array with FNBW = 10°.

$$\alpha_k = \delta^{1/k}\alpha_{k-1}, \tag{10}$$

where $\delta = 5.6 \times 10^{-3}$.

(e) *Selection*: To decide whether or not the new solution should be a member of next generation, it is compared with the present one using greedy criterion. The solution yielding the lower fitness value survives for the next generation.

4. Simulation results

We consider a uniform concentric two-ring array with 35 and 70 elements in the two successive concentric ring with the fixed inter element spacing $d_m = \lambda/2$.

It is possible to lower side lobes by turning off selected elements in the uniform array. Some elements within a ring are turned off or effectively removed from the ring in order to modify the current density on the aperture. The goal is to minimize the maximum side lobe level by creating a low side lobe density taper on the array aperture.

Various global optimizers are used in different literatures to perform the thinning of the array [12–18]. We applied FFA to optimize the proposed designing problem. In the first example, the uniformly weighted array uses 34.29% thinning to reduce the SLL to −18.36 dB. FNBW is not allowed to exceed the value of 10°. Distributions of turned on and turned off elements in both the rings are shown in Table 1. Figure 2 presents normalized power pattern of the thinned two-ring array having FNBW = 10°. Convergence characteristic of FFA applied to solve the design problem is shown in Figure 3.

In the next example, FFA is applied to compute the distributions of the turned on and turned off elements along with the non-uniform excitations applied on the turned on elements. Use of non-uniform excitations reduces the SLL to −18.71 dB for same FNBW using 25.71% thinning. Distributions of turned on and turned off elements and the non-uniform amplitude excitations on the turned on elements in both the rings are shown in

Table 1: Case 1. Distribution of the turned on and turned off elements of the uniformly excited thinned two-ring array with FNBW = 10° ('1' for turned ON and '0' for turned OFF).

Ring number	Distribution of ON and OFF element
1	0, 1, 0, 1, 1, 1, 1, 1, 1, 1, 1, 0, 1, 0, 1, 1, 0, 0, 0, 0, 0, 0, 1, 1, 0, 1, 1, 0, 1, 1, 1, 1, 0, 1, 0
2	1, 1, 0, 1, 0, 1, 0, 1, 1, 1, 0, 1, 0, 0, 1, 1, 1, 1, 1, 0, 1, 1, 1, 1, 1, 1, 0, 1, 1, 0, 0, 1, 0, 1, 1, 0, 1, 0, 0, 1, 0, 1, 1, 1, 1, 1, 0, 1, 1, 1, 1, 1, 1, 1, 0, 1, 1, 0, 1, 1, 1, 1, 1, 0, 1, 0, 1, 0, 0, 1

Table 2: Case 2. Distribution of the turned on and turned off elements of the non-uniformly excited thinned two-ring array with FNBW = 10°.

Ring number	Distribution of ON and OFF element
1	1, 0, 1, 0, 1, 1, 0, 0, 1, 1, 1, 1, 1, 1, 0, 1, 1, 1, 0, 0, 1, 1, 0, 1, 1, 1, 1, 1, 1, 0, 1, 1, 0, 1, 1
2	1, 0, 0, 0, 0, 1, 1, 1, 1, 1, 1, 1, 1, 1, 1, 1, 1, 1, 1, 1, 1, 1, 1, 0, 1, 0, 0, 1, 0, 0, 0, 0, 1, 1, 1, 1, 0, 1, 0, 1, 1, 1, 1, 1, 1, 1, 1, 0, 1, 1, 1, 1, 1, 1, 1, 0, 1, 1, 1, 1, 1, 0, 1, 1, 1, 1, 1, 0, 1

Table 3: Case 2. Non-uniform amplitude distribution of the thinned two-ring array with FNBW = 10°.

Ring no.	Current amplitude distribution
1	0.30771, 0, 0.58833, 0, 0.62705, 0.48121, 0, 0, 0.3116, 0.67848, 0.45069, 0.66146, 0.30018, 0.58793, 0, 0.47253, 0.54168, 0.33669, 0, 0, 0.59626, 0.53515, 0, 0.78959, 0.48638, 0.64971, 0.8674, 0.27636, 0.99964, 0, 0.59577, 0.26738, 0, 0.13901, 0.29765
2	0.67513, 0, 0, 0, 0, 0.76981, 0.73805, 0.69748, 0.4967, 0.85739, 0.5447, 0.24163, 0.37219, 0.4286, 0.64008, 0.43694, 0.65127, 0.63139, 0.89873, 0.42095, 0.41357, 0.48873, 0.25799, 0.67997, 0, 0.81114, 0, 0, 0.38026, 0, 0, 0, 0, 0.9501, 0.61723, 0.71006, 0.79899, 0, 0.27174, 0, 0.56569, 0.88156, 0.61673, 0.72165, 0.36353, 0.58794, 0.39542, 0.66902, 0, 0.13826, 0.54412, 0.61824, 0.48088, 0.91006, 0.56589, 0.49571, 0, 0.28128, 0.63783, 0.5846, 0.3958, 0.35549, 0, 0.40529, 0.31662, 0.53309, 0.57791, 0.3524, 0, 0.41432

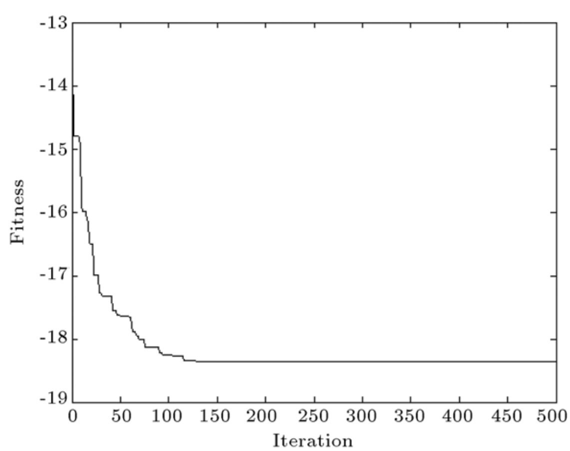

Figure 3: Convergence curve of the thinned two-ring array with FNBW = 10° using FFA.

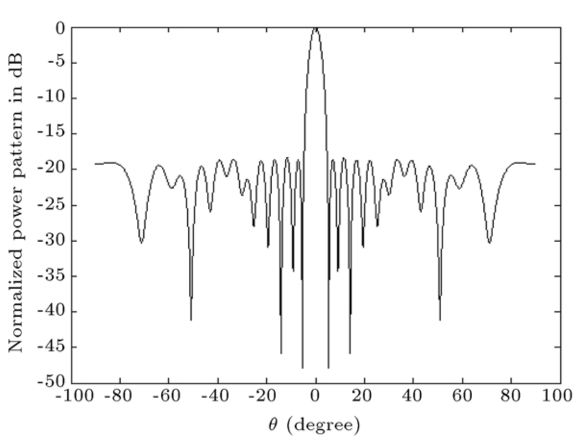

Figure 4: Normalized power pattern of the non-uniformly excited thinned two-ring array with FNBW = 10°.

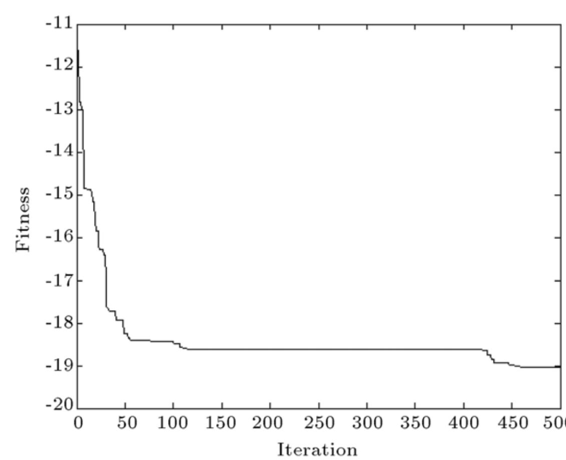

Figure 5: Convergence curve of the non-uniformly excited thinned two-ring array with FNBW = 10° using FFA.

Tables 2 and 3, respectively. Figure 4. presents the normalized power pattern with FNBW = 10°. Convergence rate of FFA to optimize the array is shown in Figure 5.

Next example considers the same designing instances. However, FNBW of the main beam is allowed to increase up to 20. FFA is applied to compute the distributions of the turned on and turned off elements along with the non-uniform excitations on the turned on elements. Radiation patterns are generated with SLL equal to −34.13 dB and FNBW = 16°. The percentage of thinning obtained in this case is 31.43. Distributions of turned on and turned off elements and the non-uniform amplitude excitations on the turned on elements in both the rings are shown in Tables 4 and 5, respectively. Figure 6 presents the normalized power pattern with FNBW = 10°. Fitness evaluation in iterations using FFA is shown in Figure 7.

Finally, the array is optimally thinned to minimize SLL for FNBW = 10°. Desired value of thinning is fixed at 50%. FFA is applied to compute the distributions of the turned on and turned off elements along with the non-uniform excitations on

Table 4: Case 3. Distribution of the turned on and turned off elements of the non-uniformly excited thinned two-ring array with FNBW = 16°.

Ring number	Distribution of ON and OFF element
1	0, 1, 0, 1, 1, 1, 1, 1, 1, 1, 0, 1, 1, 1, 1, 1, 1, 1, 0, 1, 1, 1, 1, 1, 1, 1, 1, 1, 1, 1, 1, 1, 0, 1, 1
2	1, 0, 0, 0, 1, 1, 1, 1, 1, 1, 1, 0, 1, 1, 1, 1, 1, 1, 1, 1, 0, 0, 0, 1, 1, 1, 1, 1, 0, 1, 0, 1, 0, 0, 0, 0, 0, 0, 1, 0, 0, 1, 1, 1, 1, 1, 0, 0, 1, 1, 1, 1, 1, 0, 1, 0, 1, 1, 0, 1, 0, 1, 0, 0, 1, 0, 0, 1, 0, 1

Table 5: Case 3. Non-uniform amplitude distribution of the thinned two-ring array with FNBW = 16°.

Ring no.	Current amplitude distribution
1	0, 0.21598, 0, 0.56622, 0.52728, 0.41041, 0.93596, 0.7819, 0.32914, 0.8173, 0, 0.41365, 0.48089, 0.49829, 0.77783, 0.42288, 0.023187, 0.38612, 0, 0.092517, 0.56358, 0.68976, 0.69798, 0.58213, 0.57946, 0.67366, 0.56302, 0.42039, 0.6908, 0.68383, 0.36315, 0.061874, 0, 0.76401, 0.58086
2	0.17404, 0, 0, 0, 0.57674, 0.13696, 0.10585, 0.50758, 0.5008, 0.71481, 0.68482, 0, 0.58251, 0.59068, 0.54414, 0.99419, 0.94093, 0.36054, 0.61427, 0.57982, 0, 0, 0, 0.49137, 0.47354, 0.045567, 0.34818, 0.25925, 0, 0.24005, 0, 0.013554, 0, 0, 0, 0, 0, 0, 0.36999, 0, 0, 0.32734, 0.21101, 0.35607, 0.56646, 0.41375, 0, 0, 0.53221, 0.90953, 0.66238, 0.97999, 0.59649, 0, 0.79278, 0, 0.63605, 0.46694, 0, 0.85007, 0, 0.67382, 0, 0, 0.27819, 0, 0, 0.010082, 0, 0.1979

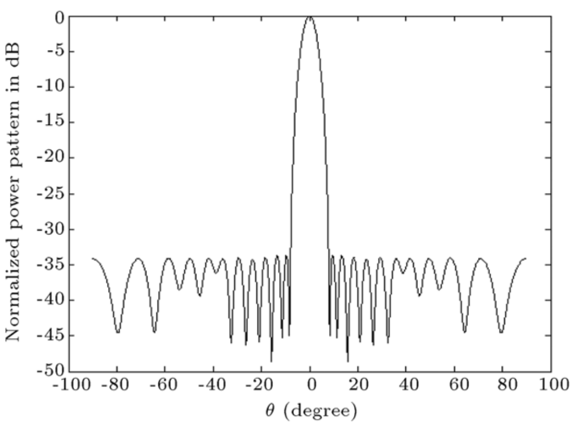

Figure 6: Normalized power pattern of the non-uniformly excited thinned two-ring array with FNBW = 16°.

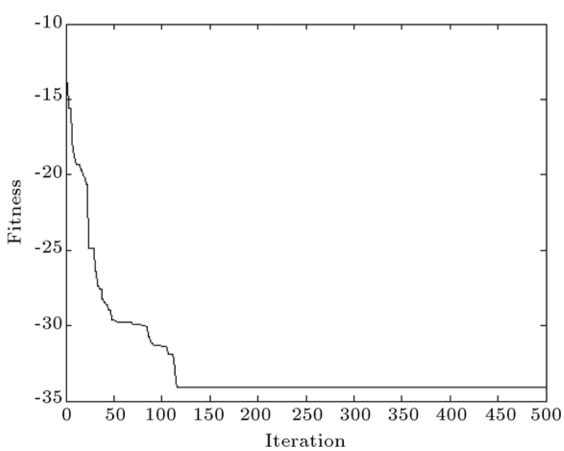

Figure 7: Convergence curve of the non-uniformly excited thinned two-ring array with FNBW = 16° using FFA.

the turned on elements. Radiation patterns are generated with SLL equal to −18.67 dB and FNBW = 10°. The percentage of thinning obtained is 50.47. Distributions of turned on and turned off elements and the non-uniform amplitude excitations on the turned on elements in both rings are shown in Tables 6 and 7, respectively. Figure 8 presents the normalized power pattern with FNBW = 10°. Convergence characteristic of FFA to optimize the thinned array is shown in Figure 9.

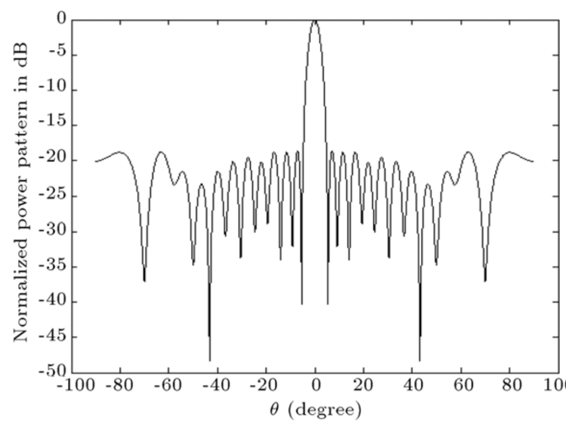

Figure 8: Normalized power pattern of the non-uniformly excited 50% thinned two-ring array with FNBW = 10°.

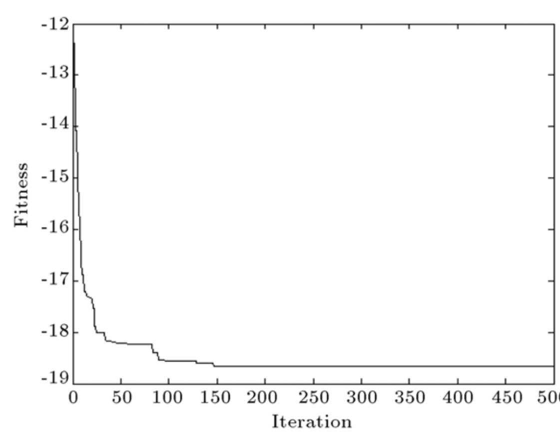

Figure 9: Convergence curve of the non-uniformly excited 50% thinned two-ring array with FNBW = 10°.

Table 8 presents the results obtained from the four designing instances.

The control parameters for FFA are set as suggested by the article [14–16]: The maximum attractiveness β_0 is set at 1. We use a time varying algorithm parameter α with initial value 0.25. Absorption coefficient γ is set at 1. Algorithm is run for 500 iterations. A swarm size of 50 is used for the experiment and the dynamic range of the search space is bounded within (0, 1). Patterns are approximated with 1° step size in each case.

Table 6: Case 4. Distribution of the turned on and turned off elements of the non-uniformly excited 50% thinned two-ring array with FNBW = 10°.

Ring number	Distribution of ON and OFF element
1	0, 0, 0, 0, 1, 0, 0, 0, 0, 0, 1, 1, 1, 0, 1, 1, 1, 0, 0, 1, 0, 1, 0, 1, 0, 1, 1, 1, 0, 0, 1, 0, 0, 0, 1
2	1, 1, 1, 0, 0, 0, 1, 1, 0, 1, 0, 1, 1, 0, 1, 1, 0, 1, 0, 1, 1, 1, 1, 1, 1, 1, 1, 0, 1, 0, 0, 0, 0, 0, 1, 0, 1, 0, 0, 1, 1, 0, 0, 0, 1, 0, 0, 0, 1, 0, 1, 1, 1, 1, 1, 0, 1, 1, 1, 0, 1, 0, 1, 1, 0, 0, 0, 0, 0, 0

Table 7: Case 4. Non-uniform amplitude distribution of the 50% thinned two-ring array with FNBW = 10°.

Ring no.	Current amplitude distribution
1	0, 0, 0, 0, 0.91019, 0, 0, 0, 0, 0, 0.44281, 0.34973, 0.27398, 0, 0.19646, 0.43647, 0.15193, 0, 0, 0.53358, 0, 0.2912, 0, 0.54008, 0, 0.22055, 0.69045, 0.53065, 0, 0, 0.77276, 0, 0, 0, 0.40488
2	0.86562, 0.85482, 0.39831, 0, 0, 0, 0.34946, 0.63776, 0, 0.94188, 0, 0.3795, 0.013577, 0, 0.90461, 0.42448, 0, 0.34739, 0, 0.49672, 0.60214, 0.50108, 0.38823, 0.60306, 0.50682, 0.56798, 0.68162, 0, 0.42545, 0, 0, 0, 0, 0, 0.99885, 0, 0.71622, 0, 0, 0.29923, 0.64827, 0, 0, 0, 0.5756, 0, 0, 0, 0.63711, 0, 0.9671, 0.88918, 0.9927, 0.6239, 0.46681, 0, 0.59254, 0.14871, 0.87285, 0, 0.74311, 0, 0.11505, 0.92346, 0, 0, 0, 0, 0, 0

Table 8: Results obtained using thinned two-ring array.

Design parameters	Proposed thinned array with FNBW constraint			
	Case 1 Thinned arrays with unity excitation amplitude and fixed FNBW	Case 2 Thinned arrays with tapering excitation amplitude and fixed FNBW	Case 3 Thinned arrays with tapering excitation amplitude and wider FNBW	Case 4 50% thinned arrays with tapering excitation amplitude and fixed FNBW
Percentage of thinning	34.29	25.71	31.43	50.47
Side lobe level (dB)	−18.36	−18.71	−34.13	−18.67
First null beam width (°)	10	10	16	10

We again apply two more state-of-the-art meta-heuristics like PSO and DE [9–12] in an attempt to make a fair comparison among the algorithms regarding their performances. The algorithms are allowed to run for a similar number of function evaluation (as used in FFA) and applied on a single instantiation of the design problem of the unequally excited thinned two-ring Uniform Concentric Circular Arrays (UCCA).

Tables 9–12 presents the amplitude and switching distributions in each case using PSO and DE.

Comparative results obtained using PSO, DE and FFA is shown in Table 13.

Table 14 compares the quality of the optimal solutions achieved in terms of the mean and standard deviation of the best results for 20 independent run using PSO, DE and FFA. As the distributions of the best objective function values do not follow a normal distribution, the Wilcoxon two-sided rank sum test [11,19] was performed to compare the objective function mean value, standard deviation and P value of each algorithm. Table 14 shows FFA produces smaller mean cost values. So we consider FFA as the best performing algorithm. P values obtained through the rank sum test between the best algorithm and each of the contestants are less than 0.05, so the null hypothesis is rejected at the 5% significance level. It indicates that the better final cost value achieved by the best algorithm in each case is statistically significant and does not occur by chance. Here NA stands for "Not Applicable" and it occurred for the best performing algorithm.

Figures 10 and 11 present the corresponding radiation patterns using PSO and DE.

Convergence characteristics of PSO and DE over the referred designing instance are plotted in Figures 12 and 13. It is seen that FFA takes less computation time to the reach minimum cost function value compared to that of PSO and DE.

The parameters for PSO and DE are set following the guidelines provided in [9–12]. The parametric setup for all the algorithms is shown in Table 15.

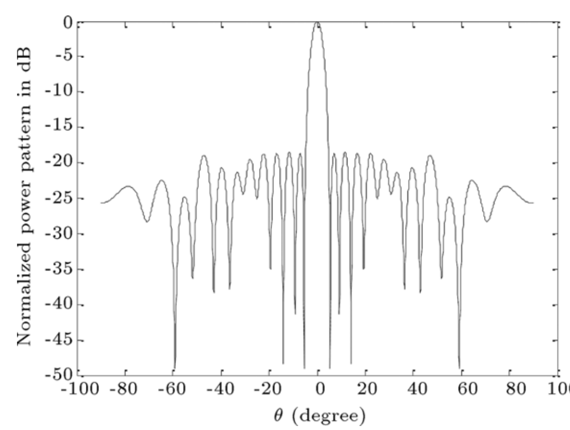

Figure 10: Normalized power pattern of the non-uniformly excited thinned two-ring array with FNBW = 10° using PSO.

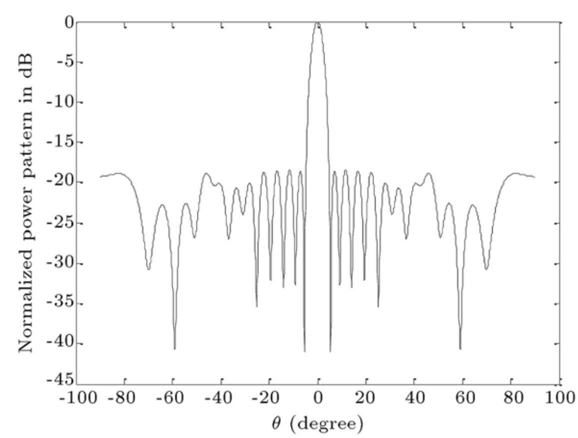

Figure 11: Normalized power pattern of the non-uniformly excited thinned two-ring array with FNBW = 10° using DE.

Table 9: Non-uniform amplitude distribution of the thinned two-ring array with FNBW = 10° using PSO.

Ring no.	Current amplitude distribution
1	0.614884633914935, 0, 0.609048646365958, 0.438002860892190, 0.504750984922368, 0.565500957201704, 0.448508282055358, 0, 0.691034049293430, 0, 0.518727125389874, 0.129534471749535, 0, 0, 0, 0.336723571589926, 0.200338847013540, 0, 0.691779587797087, 0, 0, 0.825749201231510, 0, 0.584511963242304, 0.702211959539823, 0.673774023875891, 0, 0.472214136530467, 0, 0, 0.644330291428110, 0, 0, 0, 0.338064141273896,
2	0.543738035327952, 0.311840676370408, 0, 0.219244261507038, 0.113362292174136, 0.682964950471427, 0.482015431602514, 0, 0.552596791347408, 0.385378772133575, 0.382092032769983, 0, 0.365772313101982, 0.457224977975200, 0.585486174303804, 0, 0.601015292081740, 0.491857787405195, 0.623257534305018, 0.180208543472072, 0, 0.389964815238378, 0.726935792071434, 0.513339671100907, 0.575076170284705, 0.423321433491466, 0.649617763721403, 0.710944176576369, 0.526809630328404, 0.339711089893135, 0, 0.592141726762528, 0.546121679279286, 0, 0, 0.397425123680237, 0.421915031392375, 0.164822184928914, 0, 0, 0.273928088793042, 0, 0, 0.410110001095708, 0.387679639391263, 0, 0.319118836781262, 0.164815333350100, 0.971751689794834, 0.262229701095854, 0.638423442951124, 0, 0.970099640361922, 0.469430266187169, 0.563442090497217, 0.522361930332119, 0, 0, 0.548124523083358, 0.248544910733047, 0.871163764348117, 0.325365014237093, 0, 0.405193314294744, 0, 0, 0, 0.395466886360039, 0.749955272584877, 0.175266571293829

Table 10: Distribution of the turned on and turned off elements of the non-uniformly excited thinned two-ring array with FNBW = 10° using PSO.

Ring number	Distribution of ON and OFF element
1	1, 0, 1, 1, 1, 1, 1, 0, 1, 0, 1, 1, 0, 0, 0, 1, 1, 0, 1, 0, 0, 1, 0, 1, 1, 1, 0, 1, 0, 0, 1, 0, 0, 0, 1,
2	1, 1, 0, 1, 1, 1, 1, 0, 1, 1, 1, 0, 1, 1, 1, 0, 1, 1, 1, 1, 0, 1, 1, 1, 1, 1, 1, 1, 1, 1, 0, 1, 1, 0, 0, 1, 1, 1, 0, 0, 1, 0, 0, 1, 1, 0, 1, 1, 1, 1, 1, 0, 1, 1, 1, 1, 0, 0, 1, 1, 1, 1, 0, 1, 0, 0, 0, 1, 1, 1

Table 11: Non-uniform amplitude distribution of the thinned two-ring array with FNBW = 10° using PSO.

Ring no.	Current amplitude distribution
1	0, 0.147883291848155, 0, 0, 0.530572656769734, 0.457770055234213, 0.453080820046912, 0.923899428842188, 0.889592787971865, 0.275708471234319, 0.530551356019208, 0.658700869926763, 0.626525260919294, 0, 0.248378893505449, 0.234353111018470, 0.720643481302828, 0.445530310436100, 0, 0, 0.599313783560956, 0.553208869788395, 0.775787484995688, 0.116758550855016, 0.570013346820740, 0.850862957535496, 0.790053774409646, 0.649959855497000, 0.0552841630442377, 0.282100004035401, 0.327025496377715, 0.809567539218435, 0, 0.495373099588240, 0.546452208373556,
2	0, 0, 0.140561288427447, 0, 0.412767385334919, 0.338511895996380, 0.556598323864951, 0.576667565177736, 0.441522644108446, 0.607952705635485, 0.818075437556334, 0, 0.470823497214985, 0.802017365579175, 0, 0.414927451729587, 0.729275459864935, 0.326817986710711, 0, 0.752881972996409, 0, 0, 0.471460212163684, 0.213202058566403, 0.795670546865239, 0.187819326765135, 0.382452993528900, 0.752949828877628, 0.550678254865560, 0.457662065438889, 0, 0, 0.696786495210555, 0.124261401138325, 0.992216940468477, 0.354505566577801, 0.406822526844560, 0, 0.546237699432227, 0, 0, 0, 0.733166208767503, 0.656368994530841, 0.890083048588317, 0.626794539919672, 0.348627316324089, 0, 0, 0.851953364235197, 0.944571298050550, 0, 0, 0.385585163707374, 0.976541276324625, 0.558677963769360, 0.836513980847818, 0, 0, 0.609345370260591, 0.0982359808277783, 0.403558620324959, 0, 0.864677403806827, 0.362146282314124, 0.123574708371613, 0, 0.664302433941419, 0.484633340909298, 0.761706681269439

Table 12: Distribution of the turned on and turned off elements of the non-uniformly excited thinned two-ring array with FNBW = 10° using DE.

Ring number	Distribution of ON and OFF element
1	0, 1, 0, 0, 1, 1, 1, 1, 1, 1, 1, 1, 1, 0, 1, 1, 1, 1, 0, 0, 1, 1, 1, 1, 1, 1, 1, 1, 1, 1, 1, 1, 0, 1, 1
2	1, 0, 0, 1, 0, 1, 1, 1, 1, 1, 1, 1, 0, 1, 1, 0, 1, 1, 1, 0, 1, 0, 0, 1, 1, 1, 1, 1, 1, 1, 1, 0, 0, 1, 1, 1, 1, 1, 0, 1, 0, 0, 0, 1, 1, 1, 1, 1, 0, 0, 1, 1, 0, 0, 1, 1, 1, 1, 0, 0, 1, 1, 1, 0, 1, 1, 1, 0, 1, 1

Table 13: Comparative results using PSO, DE and FFA.

Algorithmes	PSO	DE	FFA
Percentage of thinning	29	24.76	25.71
Side lobe level (dB)	−18.38	−18.44	−18.71
First null beam width (°)	10	10	10

Table 14: Mean cost values, standard deviations and P values.

Algorithms	PSO	DE	FFA
Mean cost function	−17.93	−18.07	−18.33
Standard deviation	0.2900	0.2432	0.2219
P-value	1.7936e−004	0.0032	NA

5. Conclusions

The paper describes the method of thinning of concentric two-ring array of isotropic elements to reduce side lobe level for specific first null beam width. The performances of the four design instances are illustrated in a precise fashion.

Results show that the thinning of an array makes it aperiodic so a true grating lobe never appears. Suitable thinning limits the cost of beam-forming network and reduces the power consumption of the antenna system.

It is observed that the use of non-uniform amplitude weight in the thinned array reduces the SLL more effectively. However, the designing problems using non-uniform amplitude weight require more optimization variables and takes longer execution time to converge to a good solution than the first approach. Application of non-uniform excitations compounds the complexity of the beam-forming network.

It has been noticed that increasing the FNBW can significantly enhance the SLL performances. Moreover, to increase the power efficiency we may fix the percentage of

Table 15: Parametric set up of different algorithms.

PSO		DE		FFA	
Parameter	Value	Parameter	Value	Parameter	Value
Population size	50	Population size	60	Swarm size	50
c_1, c_2	1.49	F	0.8	β_0, γ	1
w	Linearly varies from 0.9 to 0.4	Cr	0.9	α	0.25
Max cycle	500	Max cycle	1000	Max cycle	500
Total function evaluations	25 000	Total function evaluations	25 000	Total function evaluations	25 000

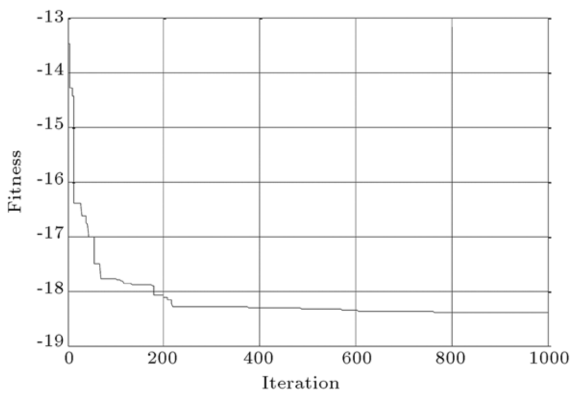

Figure 12: Convergence curve of the thinned two-ring array with FNBW = 10° using PSO.

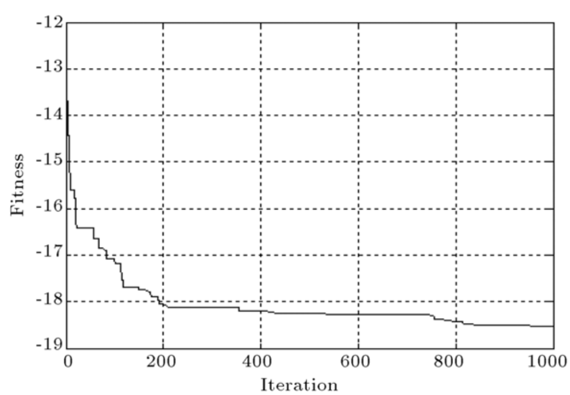

Figure 13: Convergence curve of the thinned two-ring array with FNBW = 10° using DE.

thinning at a higher value with little compromise on the design specifications.

Proposed technique is capable of optimizing more complex geometries and therefore is suitable for many applications in mobile and wireless communication area. The design results using fire fly algorithm comfortably beat other state-of-the-art meta-heuristics like PSO and DE those are frequently used in most of the published articles of recent times.

References

[1] Haupt, R.L. "Thinned arrays using genetic algorithms", *IEEE Transactions on Antennas and Propagation*, 42(7), pp. 993–999 (1994).

[2] Keizer, W.P.M.N. "Linear array thinning using iterative FFT techniques", *IEEE Transactions on Antennas and Propagation*, 56(8), pp. 2757–2760 (2008).

[3] Stearns, C. and Stewart, A. "An investigation of concentric ring antennas with low sidelobes", *IEEE Transactions on Antennas and Propagation*, 13(6), pp. 856–863 (1965).

[4] Goto, N. and Cheng, D.K. "On the synthesis of concentric-ring arrays", *Proceedings of the IEEE*, 58(3), pp. 839–840 (1970).

[5] Dessouky, M.I., Sharshar, H.A. and Albagory, Y.A. "Efficient sidelobe reduction technique for small-sized concentric circular arrays", *Progress in Electromagnetics Research*, 65, pp. 187–200 (2006).

[6] Fallahi, R. and Roshandel, M. "Effect of mutual coupling and configuration of concentric circular array antenna on the signal-to-interference performance in CDMA systems", *Progress in Electromagnetics Research*, 76, pp. 427–447 (2007).

[7] Yan, K.K. and Yilong, L. "Sidelobe reduction in array-pattern synthesis using genetic algorithm", *IEEE Transactions on Antennas and Propagation*, 45(7), pp. 1117–1122 (1997).

[8] Mangoud, M.A.A. and Elragal, H.M. "Antenna array pattern synthesis and wide null control using enhanced particle swarm optimization", *Progress in Electromagnetics Research B*, 17, pp. 1–14 (2009).

[9] Pathak, N., Basu, B. and Mahanti, G.K. "Combination of inverse fast Fourier transform and modified particle swarm optimization for synthesis of thinned mutually coupled linear array of parallel half-wave length dipoles antennas", *Progress in Electromagnetics Research M*, 16, pp. 105–115 (2011).

[10] Roy, G.G., Das, S., Chakraborty, P. and Suganthan, P.N. "Design of non-uniform circular antenna arrays using a modified invasive weed optimization algorithm", *IEEE Transactions on Antennas and Propagation*, 59(1), pp. 110–118 (2011).

[11] Panduro, M.A., Brizuela, C.A., Balderas, L.I. and Acosta, D.A. "A comparison of genetic algorithms, particle swarm optimization and the differential evolution method for the design of scanable circular antenna arrays", *Progress in Electromagnetics Research B*, 13, pp. 171–186 (2009).

[12] Haupt, R.L. "Thinned concentric ring array", *Proc. IEEE Antennas Propagation Int. Symp.*, San Diego, CA, pp. 1–4 (2008).

[13] Pathak, N., Nanda, P. and Mahanti, G.K. "Synthesis of thinned multiple concentric circular ring array antennas using particle swarm optimization", *Journal of Infrared, Millimeter and Terahertz Waves*, 30(7), pp. 709–716 (2009).

[14] Basu, B. and Mahanti, G.K. "Fire fly and artificial bees colony algorithm for synthesis of scanned and broadside linear array antenna", *Progress in Electromagnetics Research B*, 32, pp. 169–190 (2011).

[15] Yang, X.S., *Nature-Inspired Metaheuristic Algorithms*, Luniver Press, UK pp. 79–86 (2008).

[16] Szymon, L. and Slawomir, Z. "Firefly algorithm for continuous constrained optimization tasks", *Lecture Notes in Computer Science*, 5796, pp. 97–106 Springerlink (2009).

[17] Elliott, R.S., *Antenna Theory and Design*, revised Edn., Wiley Interscience, New Jersey pp. 196–265 (2003).

[18] Chatterjee, A., Mahanti, G.K. and Pathak, N.N. "Comparative performance of gravitational search algorithm and modified particle swarm optimization algorithm for synthesis of thinned scanned concentric ring array antenna", *Progress in Electromagnetics Research B*, 25, pp. 331–348 (2010).

[19] Gibbons, J.D. and Chakraborti, S., *Nonparametric Statistical Inference*, 3rd rev/ex Edn., CRC Press, New York pp. 156–393 (1985).

Banani Basu obtained her B.E. and M.Tech. degrees in Electronics and Communication Engineering from Jalpaiguri Government Engineering College, India, and WB University of Technology, India, in 2004 and 2008, respectively. She received her Ph.D. degree from National Institute of Technology, Durgapur, in 2012. Presently, she is serving as an Assistant Professor in the department of Electronics and Communication Engineering in National Institute of Technology, Arunachal Pradesh, India. Her research interest includes Array Antenna synthesis, Soft Computing & Electromagnetics. She has published 8 research papers in international journal of repute and 6 papers in conferences.

Gautam Kumar Mahanti was born in the year 1967 in India. He obtained his Ph.D. (Engg.) from IIT, Kharagpur, India. He has more than 20 years of teaching experience. He is presently a professor in the department of Electronics and Communication Engineering, NIT, Durgapur, India. He has published 24 research papers in international journals and 21 papers in national and international conferences. He is the reviewer of many international journals like Electronics Letter, IEEE Antennas and Wireless Propagation Letter, Progress in Electromagnetics Research etc. and many conferences. He is also the program committee member of many national conferences. His biography is listed in Marqui's Who is Who in the world. His research area is Array Antenna Synthesis, Evolutionary Algorithms & Electromagnetics.